

Explanation of the cw operation of the Er³⁺ 3-μm crystal laser

M. Pollnau, Th. Graf, J. E. Balmer, W. Lüthy, and H. P. Weber

Institute of Applied Physics, University of Bern, Sidlerstrasse 5, CH-3012 Bern, Switzerland

(Received 14 October 1993; revised manuscript received 5 January 1994)

A computer simulation of the Er³⁺ 3-μm crystal laser considering the full rate-equation scheme up to the ⁴F_{7/2} level has been performed. The influence of the important system parameters on lasing and the interaction of these parameters has been clarified with multiple-parameter variations. Stimulated emission is fed mainly by up-conversion from the lower laser level and in many cases is reduced by the quenching of the lifetime of this level. However, also without up-conversion a set of parameters can be found that allows lasing. Up-conversion from the upper laser level is detrimental to stimulated emission but may be compensated by cross relaxation from the ⁴S_{3/2} level. For a typical experimental situation we started with the parameters of Er³⁺:LiYF₄. In addition, the host materials Y₃Al₅O₁₂ (YAG), YAlO₃, Y₃Sc₂Al₃O₁₂ (YSGG), and BaY₂F₈, as well as the possibilities of codoping, are discussed. In view of the consideration of all excited levels up to ⁴F_{7/2}, all lifetimes and branching ratios, ground-state depletion, excited-state absorption, three up-conversion processes as well as their inverse processes, stimulated emission, and a realistic resonator design, this is, to our knowledge, the most detailed investigation of the Er³⁺ 3-μm crystal laser performed so far.

PACS number(s): 42.55.Rz, 42.60.Lh, 78.45.+h

I. INTRODUCTION

In recent years there has been an enormous theoretical and practical interest in the Er³⁺ 3-μm laser. Its possible application in surgery due to the high absorption of the 3-μm wavelength in water evoked experimental efforts to increase the power and efficiency of the laser output and to construct compact systems [1-12]. The processes leading to continuous inversion on a transition, which can be self-terminating due to the longer lifetime of the lower laser level, have been studied by spectroscopic investigations and computer simulations [1-17].

Despite several attempts made to understand cw operation on a self-terminating transition, there has as yet been no full explanation of the Er³⁺ 3-μm laser. Possible reasons for the occurrence of cw laser operation proposed so far are (see Fig. 1) (i) depletion of the lower laser level due to excited-state absorption (ESA) ⁴I_{13/2} → ²H_{11/2} at the 795-nm pump wavelength [8], (ii) a distribution of the excitation of the ⁴S_{3/2} and ²H_{11/2} levels into the laser levels due to the cross-relaxation process (⁴S_{3/2} + ²H_{11/2}, ⁴I_{15/2}) → (⁴I_{9/2}, ⁴I_{13/2}) [16] and a subsequent multiphonon decay ⁴I_{9/2} → ⁴I_{11/2}, (iii) depletion of the lower and feeding of the upper laser level due to the up-conversion process (⁴I_{13/2}, ⁴I_{13/2}) → (⁴I_{15/2}, ⁴I_{9/2}) [7,12,16,17] and a subsequent multiphonon decay ⁴I_{9/2} → ⁴I_{11/2}, and (iv) a relatively long lifetime of the upper laser level in combination with a low branching ratio from the upper to the lower laser level [14]. All these explanations, however, consider each only a single aspect and cannot describe such a complex system as Er³⁺.

In our paper, we present a computer simulation of the Er³⁺ 3-μm laser, which includes, all excited levels up to ⁴F_{7/2}, all lifetimes and branching ratios, the depletion of the ground state, excited-state absorption, three up-

conversion processes as well as their inverse processes, stimulated emission, and a realistic resonator design. Especially the inclusion of the inverse up-conversion processes gives deeper insight into the population mechanisms of the system. The goal is to predict the properties of the crystal that would lead to the best laser performance at 3 μm.

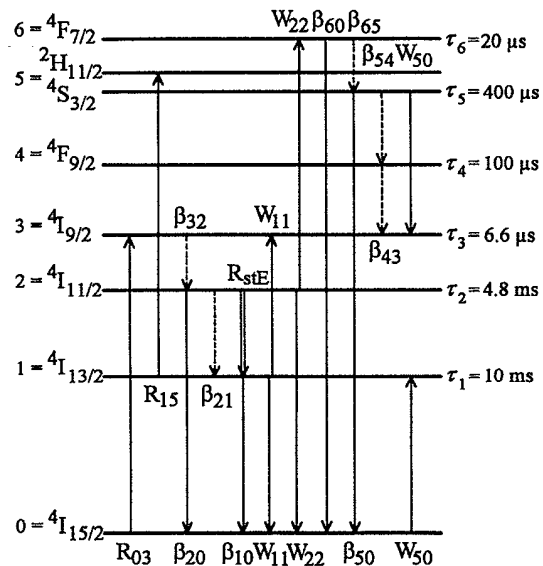


FIG. 1. Er³⁺:LiYF₄ level scheme indicating the processes which are relevant for the excitation of the laser levels. GSA (R₀₃) and ESA (R₁₅) are indicated only for the 795-nm pump wavelength. The relative rates of the processes are given in Table I.

II. RATE EQUATIONS

The labeling of the levels considers the energetic order of the Er³⁺ level system starting with 0 for the ground state; see Fig. 1. Since the ²H_{11/2} level is thermally coupled with the ⁴S_{3/2} level these are treated as a combined level with a Boltzmann-population distribution. The initial set of parameters used in our rate-equation model is taken from Er³⁺:LiYF₄, because this crystal exhibits efficient cw operation at 3 μ m when diode pumped at 795 nm into the ⁴I_{9/2} level and at 970 nm into the ⁴I_{11/2} upper laser level. The lifetimes of the levels are taken as $\tau_1=10$ ms [18], $\tau_2=4.8$ ms [5], $\tau_3=6.6$ μ s [5], $\tau_4=100$ μ s, $\tau_5=400$ μ s [18], and $\tau_6=20$ μ s. These lifetimes are the intrinsic lifetimes τ of the levels at low dopant concentration and low excitation. The quenching of the intrinsic lifetimes due to ion-ion interaction or ESA is considered in the rate equations. The radiative transition rates A_{ij} from level i into level j are known from a Judd-Ofelt calculation [19]. The radiative transitions from ⁴S_{3/2} and ²H_{11/2} are weighted with their Boltzmann contribution to level 5 at 300 K, 0.935 and 0.065, respectively, and are summed for each transition. The nonradiative transition rate $A_{i,NR}$ of level i is calculated from

$$A_{i,NR} = \tau_i^{-1} - \sum_{j=0}^{i-1} A_{ij}. \quad (1)$$

The branching ratios from level i into the next lower-lying level and into other levels are

$$\beta_{ij} = (A_{ij} + A_{i,NR}) / \tau_i^{-1} \quad \text{with } i-j=1, \quad (2)$$

$$\beta_{ij} = A_{ij} / \tau_i^{-1} \quad \text{with } i-j > 1. \quad (3)$$

The values calculated from the given lifetimes and from [19] are

$$\begin{aligned} \beta_{10} &= 1, \quad \beta_{21} = 0.387, \quad \beta_{20} = 0.613, \\ \beta_{32} &= 0.999, \quad \beta_{31} = 0, \quad \beta_{30} = 0.001, \\ \beta_{43} &= 0.903, \quad \beta_{42} = 0.006, \quad \beta_{41} = 0.004, \\ \beta_{40} &= 0.087, \quad \beta_{54} = 0.306, \quad \beta_{53} = 0.012, \\ \beta_{52} &= 0.015, \quad \beta_{51} = 0.179, \quad \beta_{50} = 0.488, \\ \beta_{65} &= 0.941, \quad \beta_{64} = 0, \quad \beta_{63} = 0.002, \\ \beta_{62} &= 0.002, \quad \beta_{61} = 0.004, \quad \beta_{60} = 0.051. \end{aligned}$$

Three ion-ion interactions as well as their inverse processes are taken into account (see Fig. 1): (⁴I_{13/2}, ⁴I_{13/2}) \leftrightarrow (⁴I_{15/2}, ⁴I_{9/2}), (⁴I_{11/2}, ⁴I_{11/2}) \leftrightarrow (⁴I_{15/2}, ⁴F_{7/2}), and (⁴S_{3/2} + ²H_{11/2}, ⁴I_{15/2}) \leftrightarrow (⁴I_{9/2}, ⁴I_{13/2}). The parameters of these processes are set to be $W_{11} = W_{11}^{-1} = 3 \times 10^{-23}$ m³s⁻¹ [5], $W_{22} = W_{22}^{-1} = 1.8 \times 10^{-23}$ m³s⁻¹ [5], and $W_{50} = W_{50}^{-1} = 2 \times 10^{-23}$ m³s⁻¹, where W_{50} already includes the fact that two indistinguishable processes contribute to this cross relaxation. The concentration dependence of these parameters observed experimentally [5,11] is not the subject of this paper. We also do not include three-ion up-conversion in our simulation, because there is little reliable data available for the parameters W_{ijk} .

The transition rates due to the quadratic interionic processes depend on the absolute values of the population densities of the initial levels which depend on pump intensity. It is therefore necessary to include a realistic resonator design in order to obtain data that refer to an experimental situation. The following set of parameters has been assumed in the simulation: crystal length $l=2$ mm, dopant concentration $N_0=2 \times 10^{21}$ cm⁻³ (15 at. % on the yttrium site), and diode pumping at $\lambda_p=795$ nm by ground-state absorption (GSA) ⁴I_{15/2} \rightarrow ⁴I_{9/2} (cross section $\sigma_{03}=5 \times 10^{-21}$ cm²) and by ESA ⁴I_{13/2} \rightarrow ⁴S_{3/2} + ²H_{11/2} (cross section $\sigma_{15}=1 \times 10^{-20}$ cm²). No significant ESA from the ⁴I_{11/2} level has been measured at 795 nm [20]. The laser transition starts from the second Stark level of ⁴I_{11/2} (Boltzmann population $b_{22}=0.200$ at 300 K and degeneracy $g_{22}=2$) and terminates in the fourth Stark level of ⁴I_{13/2} ($b_{14}=0.113, g_{14}=2$) at $\lambda_{\text{laser}}=2.81$ μ m with an emission cross section $\sigma_{21}=3 \times 10^{-20}$ cm² [6]. The relaxation on the laser transition ⁴I_{11/2} \rightarrow ⁴I_{13/2} has a spontaneous radiative fraction $\gamma_{21}=0.286$.

A confocal resonator of an optical length $l_{\text{opt}}=0.1$ m is assumed. The losses L_r due to scattering and diffraction and reabsorption losses κ are neglected. An optical power of the diode $P_{\text{in}}=5$ W cw at 795 nm is chosen in order to simulate a high-power laser. The incoupling optics transmits $\eta_T=0.8$ of the pump light into the crystal. The pump and the laser beam are assumed to have a radially homogeneous profile. The average radius of the laser beam within the crystal is $r_{\text{mode}}=250$ μ m and the overlap between pump and laser mode is $\eta_B=0.7$. Only the fraction $P_1/P=10^{-7}$ of the spontaneous emission is emitted into the laser mode. The transmission of the outcoupling mirror is $T=2\%$.

The rate equations for the population densities N_i and the photon density ϕ are then given by

$$\frac{dN_6}{dt} = \sum_{i=0}^5 R_{i6} N_i - \tau_6^{-1} N_6 + W_{22} (N_2^2 - N_0 N_6), \quad (4)$$

$$\begin{aligned} \frac{dN_5}{dt} &= \sum_{i=0}^4 R_{i5} N_i - R_{56} N_5 - \tau_5^{-1} N_5 + \beta_{65} \tau_6^{-1} N_6 \\ &\quad - W_{50} (N_5 N_0 - N_3 N_1), \end{aligned} \quad (5)$$

$$\frac{dN_4}{dt} = \sum_{i=0}^3 R_{i4} N_i - \sum_{j=5}^6 R_{4j} N_4 - \tau_4^{-1} N_4 + \sum_{i=5}^6 \beta_{i4} \tau_i^{-1} N_i, \quad (6)$$

$$\begin{aligned} \frac{dN_3}{dt} &= \sum_{i=0}^2 R_{i3} N_i - \sum_{j=4}^6 R_{3j} N_3 - \tau_3^{-1} N_3 + \sum_{i=4}^6 \beta_{i3} \tau_i^{-1} N_i, \\ &\quad + W_{50} (N_5 N_0 - N_3 N_1) + W_{11} (N_1^2 - N_0 N_3), \end{aligned} \quad (7)$$

$$\begin{aligned} \frac{dN_2}{dt} &= \sum_{i=0}^1 R_{i2} N_i - \sum_{j=3}^6 R_{2j} N_2 - \tau_2^{-1} N_2 \\ &\quad + \sum_{i=3}^6 \beta_{i2} \tau_i^{-1} N_i - 2W_{22} (N_2^2 - N_0 N_6) - R_{SE}, \end{aligned} \quad (8)$$

$$\begin{aligned} \frac{dN_1}{dt} = & R_{01}N_0 - \sum_{j=2}^6 R_{1j}N_1 - \tau_1^{-1}N_1 + \sum_{i=2}^6 \beta_{i1}\tau_i^{-1}N_i \\ & + W_{50}(N_5N_0 - N_3N_1) \\ & - 2W_{11}(N_1^2 - N_0N_3) + R_{SE}, \end{aligned} \quad (9)$$

$$\begin{aligned} \frac{dN_0}{dt} = & - \sum_{j=1}^6 R_{0j}N_0 + \sum_{i=1}^6 \beta_{i0}\tau_i^{-1}N_i \\ & - W_{50}(N_5N_0 - N_3N_1) + W_{11}(N_1^2 - N_0N_3) \\ & + W_{22}(N_2^2 - N_0N_6), \end{aligned} \quad (10)$$

$$\begin{aligned} \frac{d\phi}{dt} = & (l/l_{opt})[(P_l/P)\gamma_{21}\beta_{21}\tau_2^{-1}N_2 + R_{SE}] \\ & - \{-\ln[(1-T)(1-L_r)] + 2\kappa l\}c\phi / \{2l_{opt}\}. \end{aligned} \quad (11)$$

Equation (11) corresponds to [21] with the additional factor γ_{21} considering the fraction of spontaneous radiative transition from ${}^4I_{11/2}$ to ${}^4I_{13/2}$. The stimulated-emission rate [21] with c , the vacuum speed of light, is

$$R_{SE} = [b_{22}N_2 - (g_{22}/g_{14})b_{14}N_1]\sigma_{21}c\phi. \quad (12)$$

The equation for the pump rates [21] is extended for the possibility of ESA:

$$R_{ij} = \frac{\sigma_{ij}(\lambda_p)}{\alpha(\lambda_p)} \frac{\eta_B \eta_T \lambda_p}{hcl\pi r_{mode}^2} \{1 - \exp[-\alpha(\lambda_p)l]\} P_{in} \quad (13)$$

with

$$\alpha(\lambda_p) = \sum_{n=1}^6 \sum_{m=0}^{n-1} \sigma_{mn}(\lambda_p) N_m \quad (14)$$

and h , the Planck constant. Equation (13) holds for ground-state ($i=0$) as well as excited-state ($i>0$) absorption. It contributes to the rate equations only if σ_{ij} is chosen >0 . The absorption coefficient α of (14) is the sum of the coefficients of all ground-state and excited-state transitions at which a single pump wavelength λ_p is absorbed. The rate equations are solved in a Runge-Kutta calculation of fourth order.

III. THE $\text{Er}^{3+}:\text{LiYF}_4$ LASER

In this section the rate equations are solved for different pump wavelengths with the parameters given in Sec. II. This provides deeper insight into the population mechanisms of the laser levels of the $\text{Er}^{3+}:\text{LiYF}_4$ laser. The following lasing characteristics are predicted by the simulation: With the Er^{3+} ions pumped at 795 nm on the GSA transition ${}^4I_{15/2} \rightarrow {}^4I_{9/2}$ ($\sigma_{03} = 5 \times 10^{-21} \text{ cm}^2$) and on the ESA transition ${}^4I_{13/2} \rightarrow {}^4S_{3/2} + {}^2H_{11/2}$ ($\sigma_{15} = 1 \times 10^{-20} \text{ cm}^2$), the 3- μm laser exhibits a threshold of 0.9 W and a slope efficiency of 19%. The relatively high threshold arises due to the confocal resonator and the resulting large beam radius of 250 μm . This leads to a relatively low excitation density and therefore smaller up-conversion rates. The relatively high slope efficiency can be explained by the neglect of the losses L_r and κ .

Exciting the Er^{3+} ions at 970 nm by GSA ${}^4I_{15/2} \rightarrow {}^4I_{11/2}$ ($\sigma_{02} = 3 \times 10^{-20} \text{ cm}^2$) and ESA ${}^4I_{11/2} \rightarrow {}^4F_{7/2}$ ($\sigma_{26} = 3 \times 10^{-20} \text{ cm}^2$) leads to a 0.5-W threshold and 29% slope efficiency. This shows that direct pumping into the upper laser level is clearly favorable, in agreement with experiments [10]. Pumping directly into the lower laser level at 1530 nm leads to stimulated emission as well. This has been confirmed experimentally [2,7,9]. The simulation with a cross section $\sigma_{01} = 3 \times 10^{-20} \text{ cm}^2$ in the absence of ESA indicates that the slope efficiency is 18% with the threshold at 1.4 W. The excitation of the lower laser level is up-converted into the upper laser level via W_{11} and the subsequent multiphonon relaxation β_{32} .

We investigated the difference of the population mechanisms at the 795- and 970-nm pump wavelengths in detail. At these wavelengths high-power laser diodes are available which introduce the possibility of building an all-solid-state 3- μm laser device. The differences were investigated for the same output power, because this method is independent of all alterations that occur when changing the pump wavelength. The same output power of 0.72 W is obtained when the crystal is pumped with either 5 W at 795 nm or 3.25 W at 970 nm. In Table I the population densities of the levels and the important transition rates relative to the pump rate are presented for the 795- and 970-nm pump wavelengths under these pump conditions. In the Er^{3+} level scheme of Fig. 1 these processes are indicated for the 795-nm pump wavelength. All other rates have an efficiency of less than 1% relative to the pump rate. The rate of an inverse up-conversion process relative to the rate of the normal up-conversion process with the same parameter can be obtained by multiplying the population densities of their initial levels. With the population densities given in Table I these ratios are $W_{11}^{-1}/W_{11} = 0.54$, $W_{22}^{-1}/W_{22} = 0.40$, and $W_{50}^{-1}/W_{50} = 0.025$ in the case of 795-nm pumping. This demonstrates the necessity of considering the inverse up-conversion processes W_{11}^{-1} and W_{22}^{-1} in the rate equations. This fact has already been pointed out for W_{11}^{-1} in [1,5,12,16].

The pump efficiency at the 795-nm pump wavelength is 3.25 W/5 W = 0.65 compared to 970-nm pumping. The stimulated-emission rate is $2.61 \times 10^{28} \text{ m}^{-3} \text{ s}^{-1}$ in both cases (1.09 and 1.17, respectively, relative to the pump rate; see Table I). Three effects contribute to the reduction of the pump efficiency at 795 nm.

(i) 86% of the pump power at 795 nm versus 100% of the pump power at 970 nm is adsorbed because of the higher absorption cross section at 970 nm (reduction by a factor 0.86).

(ii) Only a fraction according to the quantum efficiency $\eta_q = 795/970 = 0.82$ of the pump power at 795 nm is deposited in the upper laser level. The rest is lost by the multiphonon relaxation ${}^4I_{9/2} \rightarrow {}^4I_{11/2}$ and contributes to the heating of the crystal (reduction by a factor 0.82).

(iii) The up-conversion processes within the Er^{3+} ions lead to different distributions of the energy in the laser levels when the pump level is changed. As shown in Table I, the population of the ${}^4I_{9/2}$ level is higher for the 795-nm pump wavelength. Therefore the inverse up-

TABLE I. Populations of the energy levels relative to the dopant concentration and transition rates relative to the pump rate at 795 nm (upper row) and 970 nm (lower row) pump wavelength.

Level	⁴ I _{15/2}	⁴ I _{13/2}	⁴ I _{11/2}	⁴ I _{9/2}	⁴ F _{9/2}	⁴ S _{3/2} + ⁴ H _{11/2}	⁴ F _{7/2}
Population	0.969	0.017	0.014	0.000 16	0.000 01	0.000 11	0.000 08
	0.974	0.014	0.012	0.000 07	0.000 01	0.000 07	0.000 06
GSA	-1.00			+1.00			
	-1.00		+1.00				
ESA		-0.04				+0.04	
			-0.01				+0.01
β_{65}						+0.31	-0.31
						+0.27	-0.27
β_{60}	+0.02						-0.02
	+0.01						-0.01
β_{54}					+0.01	-0.01	
					+0.01	-0.01	
β_{50}	+0.01					-0.01	
	+0.01					-0.01	
β_{43}				+0.01	-0.01		
				+0.01	-0.01		
β_{32}			+2.00	-2.00			
			+0.95	-0.95			
β_{21}		+0.09	-0.09				
		+0.09	-0.09				
R_{SE}		+1.09	-1.09				
		+1.17	-1.17				
β_{20}	+0.15		-0.15				
	+0.13		-0.13				
β_{10}	+0.14	-0.14					
	+0.12	-0.12					
$W_{11} + W_{11}^{-1}$	+0.67	-1.34		+0.67			
	+0.70	-1.39		+0.70			
$W_{22} + W_{22}^{-1}$	+0.34		-0.68				+0.34
	+0.27		-0.55				+0.27
$W_{50} + W_{50}^{-1}$	-0.33	+0.33		+0.33		-0.33	
	-0.25	+0.25		+0.25		-0.25	

conversion process W_{11}^{-1} is stronger, which leads to a higher excitation of the lower laser level. This reduces the stimulated-emission rate to 1.09 instead of 1.17 relative to the pump rate (reduction by a factor 0.93).

The lower absorption cross section can be compensated by choosing a longer crystal. The other disadvantages (higher pump-photon energy and the higher rate of the W_{11}^{-1} process) are specific of the 795-nm pump wavelength and cannot be removed.

IV. PARAMETER VARIATIONS AND DISCUSSION

With the parameter set given in Sec. II we performed one- and three-dimensional parameter variations as a function of P_{out} . This was done in order to investigate the influence of several parameters on the output power of the laser and the dependence of these parameters on each other. We assumed diode pumping ($P_{in}=5$ -W cw) at $\lambda_p=795$ nm by GSA $^4I_{15/2} \rightarrow ^4I_{9/2}$ ($\sigma_{03}=5 \times 10^{-21}$ cm²) and ESA $^4I_{13/2} \rightarrow ^4S_{3/2} + ^2H_{11/2}$ ($\sigma_{15}=1 \times 10^{-20}$ cm²). The parameters and their variation ranges are $\tau_1=1-15$ ms, $\tau_2=0.4-9.6$ ms, $\tau_3=0.22-22$ μ s, $\tau_4=3-300$ μ s, $\tau_5=12-1200$ μ s, $\tau_6=0.6-60$ μ s,

$W_{11}=(0.1-300 \times 10^{-24}$ m³ s⁻¹, $W_{22}=(1.8-180) \times 10^{-24}$ m³ s⁻¹, $W_{50}=(0.02-200) \times 10^{-24}$ m³ s⁻¹, and $\sigma_{15}=(0-10)^{-20}$ cm². The influence of τ_4 , τ_5 , and τ_6 was investigated in one-dimensional variations. The following three-dimensional variations were carried out: (i) $P_{out}(\tau_2, W_{11}, W_{22})$; (ii) $P_{out}(\tau_2, W_{11}, \tau_1)$; (iii) $P_{out}(\tau_2, W_{11}, \sigma_{15})$; (iv) $P_{out}(\tau_3, W_{11}, \tau_1)$; (v) $P_{out}(\tau_2, W_{50}, W_{22})$; and (vi) $P_{out}(\tau_3, W_{50}, \tau_1)$. Significant results for the dependence of the output power on these parameters are presented for the variation 5 (Fig. 2) and the variation 4 (Fig. 3). The systems Er³⁺:YAG, Er³⁺:YAIO₃, Er³⁺:YSGG, and Er³⁺:BaY₂F₈ lie within this range of parameters. The difference in laser performance of these crystals can be explained by the variations. Because of the complex relations between the processes involved in the formation of population inversion, no simple rules can be given for the cw-operating Er³⁺ 3- μ m laser. The most significant results of the variations are explained in the following subsections.

A. Excited-state absorption

Pump ESA at 795 nm on the transition $^4I_{13/2} \rightarrow ^4S_{3/2} + ^2H_{11/2}$ becomes relevant only at cross

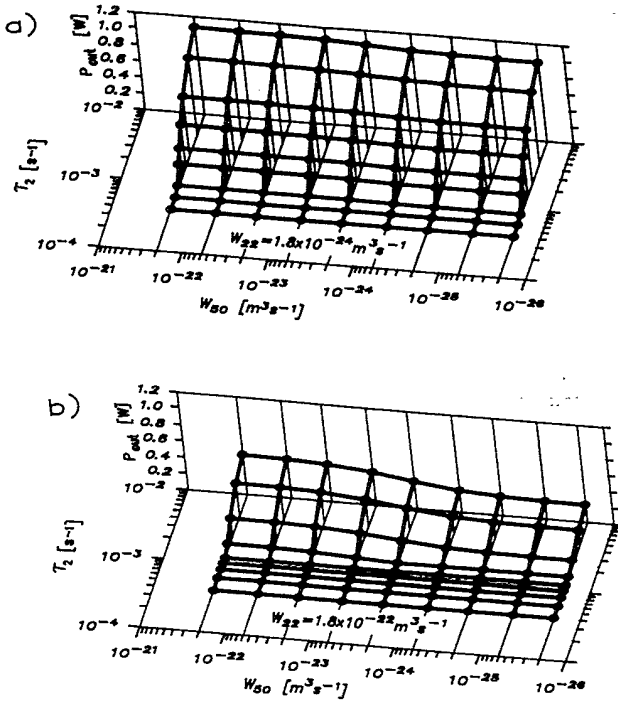


FIG. 2. Variation $P_{\text{out}}(\tau_2, W_{50}, W_{22})$: (a) $W_{22} = 1.8 \times 10^{-24} \text{ m}^3 \text{ s}^{-1}$ and (b) $W_{22} = 1.8 \times 10^{-22} \text{ m}^3 \text{ s}^{-1}$. (a) The lower limit of the lifetime τ_2 for cw operation is approximately $800 \mu\text{s}$. The cross relaxation W_{50} redistributes the energy lost by the up-conversion W_{22} into the laser levels. A larger W_{50} increases the laser output [(a) and (b), left-hand side]. (b) The effect of W_{50} increases with larger up-conversion W_{22} .

sections $\sigma_{15} > 1 \times 10^{-19} \text{ cm}^2$ which are not present in crystals such as LiYF_4 , YAG, or YAIO_3 (see, e.g., [20]). This was confirmed in the variation $P_{\text{out}}(\tau_2, W_{11}, \sigma_{15})$: The variation of σ_{15} from 0 to $1 \times 10^{-20} \text{ cm}^2$ has no effect on lasing. When raising it to $1 \times 10^{-19} \text{ cm}^2$ the laser output increases only by 5–10% depending on the other parameters. The situation may be different in YSGG [8], because ESA cross sections may be higher in this crystal.

B. Lifetime of the upper laser level

cw inversion is obtained in LiYF_4 and BaY_2F_8 in the complete absence of up-conversion processes, which can be experimentally verified with a low-doped crystal and a large pump-beam waist. In the computer simulation an output power of 0.21 W was calculated for this case. This situation has been explained by Quimby and Miniscalco [14]: In a three-level system the ratio of the populations of the upper (2) and lower (1) excited level is not simply determined by the ratio of the intrinsic lifetimes τ_i but is dependent on the feeding of level 1 through level 2:

$$N_2/N_1 = \tau_{21}/\tau_{10} = \tau_2/(\tau_1\beta_{21}). \quad (15)$$

This model applies to $\text{Er}^{3+}:\text{LiYF}_4$ with lifetimes $\tau_2 = 4.8 \text{ ms}$ and $\tau_1 = 10 \text{ ms}$ and a low branching ratio $\beta_{21} = 0.387$ from upper to lower laser level which leads to a ratio $N_2/N_1 = 1.24$ of the multiplet population densities. The

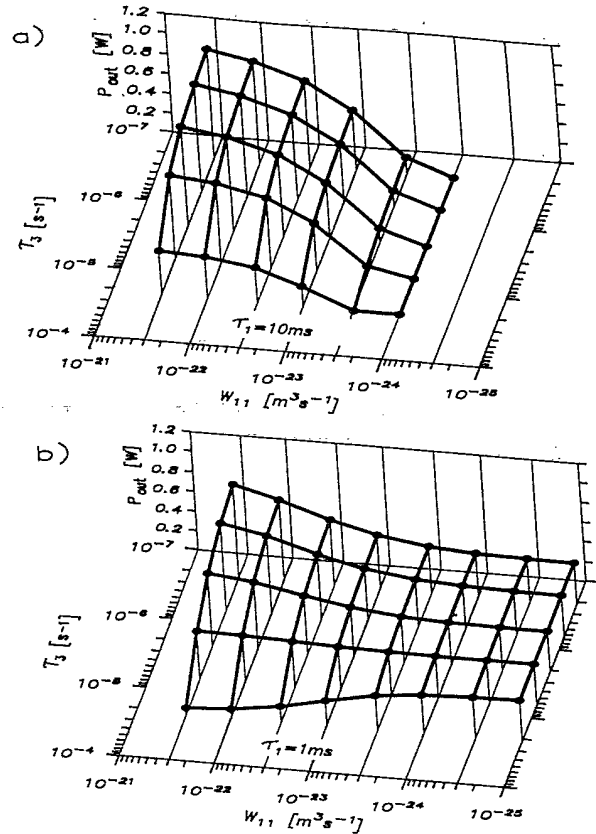


FIG. 3. Variation $P_{\text{out}}(\tau_3, W_{11}, \tau_1)$: (a) $\tau_1 = 10 \text{ ms}$ and (b) $\tau_1 = 1 \text{ ms}$. In the presence of a large up-conversion parameter W_{11} a long lifetime τ_1 increases the positive effect of W_{11} [left-hand side of (a)] and a short lifetime τ_3 decreases the inverse process W_{11}^{-1} [(a) and (b), left-hand side], both increasing laser output. With a small W_{11} parameter a short τ_1 is favorable [right-hand side of (b)], whereas τ_3 has no influence on lasing [(a) and (b), right-hand side].

ratio is even higher if the Boltzmann populations of the lasing Stark sublevels are taken into account. $\text{Er}^{3+}:\text{BaY}_2\text{F}_8$ with lifetimes $\tau_2 = 9.6 \text{ ms}$ and $\tau_1 = 10.6 \text{ ms}$ and a branching ratio $\beta_{21} = 0.35$ [11] also exhibits cw inversion without up-conversion. The situation in other crystals is different due to higher phonon energies reducing the ${}^4I_{11/2}$ lifetime and drawing the branching ratio β_{21} towards unity.

In the presence of up-conversion the lifetime of the ${}^4I_{11/2}$ upper laser level still has a large influence on laser performance. This was investigated in the variations $P_{\text{out}}(\tau_2, W_{11}, W_{22})$, $P_{\text{out}}(\tau_2, W_{11}, \tau_1)$, and $P_{\text{out}}(\tau_2, W_{50}, W_{22})$; see Fig. 2. τ_2 should be as long as possible and in the $\text{Er}^{3+}:\text{LiYF}_4$ parameter configuration there is a lower limit for τ_2 of approximately $800 \mu\text{s}$ for cw operation [see Fig. 2(a)]. This limit increases to several milliseconds when reducing W_{11} , because this reduces the depletion of the lower laser level. $\text{Er}^{3+}:\text{YAG}$ suffers from high phonon energies. This results in a low lifetime of the upper laser level ($\tau_2 = 100 \mu\text{s}$) and a

high branching ratio into the lower laser level due to multiphonon relaxation. The lower limit of τ_2 suppresses 3- μm cw lasing in Er^{3+} :YAG at 795-nm pumping.

C. Up-conversion from the laser levels

In general the inclusion of the inverse up-conversion processes is crucial for a realistic simulation of the Er^{3+} 3- μm laser. The neglect of these processes is only allowed for YAG with high phonon energies and short lifetimes of the ${}^4I_{9/2}$ and ${}^4F_{7/2}$ levels.

The up-conversion W_{11} and its influence on lasing was investigated in the variations $P_{\text{out}}(\tau_2, W_{11}, W_{22})$, $P_{\text{out}}(\tau_2, W_{11}, \tau_1)$, and $P_{\text{out}}(\tau_3, W_{11}, \tau_1)$; see Fig. 3. This process is depleting the lower and feeding the upper laser level via β_{32} . The laser exhibits a better performance when increasing W_{11} [see Fig. 3(a)]. The up-conversion W_{11} is in competition with the inverse up-conversion process W_{11}^{-1} and the 1.6- μm fluorescence β_{10} . In the presence of a large W_{11} parameter [cf. the large- W_{11} sides of Figs. 3(a) and 3(b)] the lifetime τ_3 of the terminating level of the up-conversion should be short in order to prevent the inverse process W_{11}^{-1} from increasing. In addition, τ_1 should be longer than 10 ms. Decreasing τ_1 , for example, by codoping, weakens the up-conversion W_{11} and reduces the laser output [see the large- W_{11} side of Fig. 3(b)].

In the case of a small W_{11} parameter [cf. the small- W_{11} sides of Figs. 3(a) and 3(b)] τ_3 has no influence on lasing because W_{11}^{-1} decreases with W_{11} and the rate of β_{32} is fast enough to feed stimulated emission. Maintaining a long τ_1 , thus cutting off most of the depletion of the ${}^4I_{13/2}$ level, terminates cw laser action because W_{22} is still active [see the small- W_{11} side of Fig. 3(a)]. The quenching of the lifetime of the ${}^4I_{13/2}$ level by codoping with another rare-earth metal is now favorable [see the small- W_{11} side of Fig. 3(b)]. Promising codopants are Pr^{3+} [11] and Tb^{3+} [22]. There is a combination of the lifetimes τ_1 and τ_3 , at which the processes W_{11} and W_{11}^{-1} have the same rate and the laser performance becomes independent of the magnitude of the W_{11} parameter. This is the case for $\tau_1=1$ ms and $\tau_3=7$ μs [see Fig. 3(b)]. When further reducing τ_1 or increasing τ_3 the W_{11}^{-1} process prevails over W_{11} . W_{11}^{-1} competes with β_{32} , the energy bypasses the upper laser level, and laser output is reduced with increasing W_{11} parameter [see the long- τ_3 side of Fig. 3(b)].

The influence of the up-conversion W_{22} was investigated in the variations $P_{\text{out}}(\tau_2, W_{11}, W_{22})$, $P_{\text{out}}(\tau_2, W_{50}, W_{22})$ (see Fig. 2), and $P_{\text{out}}(\tau_6)$. W_{22} is depleting the upper laser level, which reduces the laser output [cf. Figs. 2(a) and 2(b)]. The relation between the lifetime τ_6 and the up-conversion parameter W_{22} is the same as for the parameters τ_3 and W_{11} , but with the opposite effect on lasing. In the presence of a large parameter W_{22} , τ_6 should be long in order to maintain a large population in the ${}^4F_{7/2}$ level. This supports the cross relaxation W_{22}^{-1} and reduces the depletion of the upper laser level via the net sum of W_{22} and W_{22}^{-1} .

The term "self-terminating transition" should only be

used with the consideration of the depletion of the upper and lower laser levels introduced by the up-conversion rates of W_{11} and W_{22} . The up-conversion lifetime of level i due to a quadratic process is $1/(W_{ij}N_j)$. The Er^{3+} :LiYF₄ laser pumped with 5 W into the ${}^4I_{9/2}$ level (Table I) has effective lifetimes $(1/\tau_2 + W_{22}N_2)^{-1}=1.4$ ms and $(1/\tau_1 + W_{11}N_1)^{-1}=0.89$ ms in the upper and lower laser level, respectively. No self-termination of the 3- μm laser occurs in this case. The effective decay times depend on the populations of the laser levels and will change with input power, pump-beam waist, or dopant concentration. The populations of the laser levels and therefore inversion also critically depend on the energy-feeding mechanisms of the laser levels (see, e.g., [14]). This shows that the ratio of the intrinsic lifetimes of the upper and lower laser levels is not necessarily an indication for the possibility of cw lasing.

D. Cross relaxation from the ${}^4S_{3/2} + {}^2H_{11/2}$ level

Figure 2 shows the results of the parameter variation $P_{\text{out}}(\tau_2, W_{50}, W_{22})$. The cross relaxation W_{50} is fed by the up-conversion W_{22} and the subsequent multiphonon relaxation β_{65} . With the initial parameter $W_{50} (=2 \times 10^{-23} \text{ m}^3 \text{ s}^{-1})$ the depopulation of the upper laser level via W_{22} is redistributed via W_{50} into the ${}^4I_{13/2}$ and ${}^4I_{9/2}$ levels, regardless of the value of W_{22} . A further increase in W_{50} has no effect [see the large- W_{50} sides of Figs. 2(a) and 2(b)]. If W_{50} is decreased below a value of the order of $10^{-24} \text{ m}^3 \text{ s}^{-1}$, the up-converted energy is mostly lost directly to the ground state via W_{22} (${}^4I_{11/2} \rightarrow {}^4I_{15/2}$) and to ground-state fluorescence (e.g., ${}^4S_{3/2} \rightarrow {}^4I_{15/2}$) as well as multiphonon relaxations (${}^4S_{3/2} \rightarrow {}^4F_{9/2} \rightarrow {}^4I_{9/2}$). A further decrease of W_{50} again has no effect [see the small- W_{50} sides of Figs. 2(a) and 2(b)]. The difference in output power for a small and a large W_{50} is more significant if a larger part of the excitation leaves the upper laser level via W_{22} to be redistributed by W_{50} [Fig. 2(b)]. A decrease of the lifetime τ_5 introduces a relaxation channel, which is in competition with W_{50} . This leads to a decrease of the redistributed energy and a decrease of the laser output. The variation $P_{\text{out}}(\tau_3, W_{50}, \tau_1)$ exhibited no significant influence of the lifetimes τ_1 and τ_3 on W_{50} because the inverse process W_{50}^{-1} is very weak. The benefit of codoping with Cr^{3+} is present only in crystals with large W_{22} and small τ_5 such as YSGG [15] and YAG [6,13]. In this case W_{50} cannot compensate for the depletion of the upper laser level via W_{22} and redistribute the lost energy. The energy transfer from the Er^{3+} ${}^4S_{3/2}$ level via Cr^{3+} into the Er^{3+} ${}^4I_{11/2}$ and ${}^4I_{9/2}$ levels takes over the role of W_{50} .

V. CONCLUSIONS

We have developed a program for the full simulation of the erbium laser including all relevant processes and a realistic resonator design. The evaluation shows that, in the frame of the available parameters, the fluorides LiYF₄ and BaY₂F₈ are currently the best choice as host materials for the Er^{3+} 3- μm laser. The 970-nm pump wave-

length has two advantages in comparison to 795-nm pumping: It avoids the multiphonon relaxation from the $^4I_{9/2}$ level, thus increasing the quantum efficiency, and the lower population of the $^4I_{9/2}$ level reduces the inverse up-conversion from the $^4I_{9/2}$ level into the lower laser level. cw inversion can be obtained in the absence of up-conversion processes because of a long lifetime of the upper laser level and a favorable low branching ratio into the lower laser level. The strong up-conversion from the $^4I_{13/2}$ level has a major effect on stimulated emission by efficiently depleting the lower and feeding the upper laser level. In the presence of up-conversion the lifetime of the

lower laser level should be as long as possible. The quenching of this level by codoping counteracts up-conversion, thus reducing the laser output. The lifetime of the upper laser level must be longer than 800 μ s for cw-laser operation. Despite the influence of up-conversion this lifetime is the most crucial parameter for the efficient cw-laser operation of the Er^{3+} 3- μ m laser.

ACKNOWLEDGMENT

This work was supported in part by the Swiss Priority Program "Optique."

-
- [1] K. S. Bagdasarov, V. I. Zhekov, V. A. Lobachev, T. M. Murina, and A. M. Prokhorov, *Kvant. Elektron. (Moscow)* **10**, 452 (1983) [*Sov. J. Quantum Electron.* **13**, 262 (1983)].
- [2] S. A. Pollack, D. B. Chang, and N. L. Moise, *J. Appl. Phys.* **60**, 4077 (1986).
- [3] G. J. Kintz, R. Allen, and L. Esterowitz, *Appl. Phys. Lett.* **50**, 1553 (1987).
- [4] F. Auzel, S. Hubert, and D. Meichenin, *Appl. Phys. Lett.* **54**, 681 (1989).
- [5] H. Chou and H. P. Jenssen, in *Tunable Solid State Lasers*, OSA Proceeding Series, edited by M. L. Shand and H. P. Jenssen (Optical Society of America, Washington, DC, 1989), Vol. 5, pp. 167–174.
- [6] W. Shi, Ph.D. dissertation, University of Southern California, Los Angeles, 1989.
- [7] P. Xie and S. C. Rand, *Opt. Lett.* **15**, 848 (1990).
- [8] R. Clausen, G. Huber, M. A. Noginov, I. A. Shcherbakov, V. A. Smirnov, and H. Stange, in *Advanced Solid State Lasers, 1991*, Technical Digest Series (Optical Society of America, Washington, DC, 1991), pp. 172–174.
- [9] S. A. Pollack, D. B. Chang, M. Birnbaum, and M. Kokta, *J. Appl. Phys.* **70**, 7227 (1991).
- [10] R. C. Stoneman, J. G. Lynn, and L. Esterowitz, *IEEE J. Quantum Electron.* **28**, 1041 (1992).
- [11] D. S. Knowles and H. P. Jenssen, *IEEE J. Quantum Electron.* **28**, 1197 (1992).
- [12] M. Tempus, V. G. Ostroumov, W. Lüthy, H. P. Weber, and I. A. Shcherbakov, *IEEE J. Quantum Electron.* (to be published).
- [13] V. I. Zhekov, T. M. Murina, A. M. Prokhorov, M. I. Studenikin, S. Georgescu, V. Lupei, and I. Ursu, *Kvant. Elektron. (Moscow)* **13**, 419 (1986) [*Sov. J. Quantum Electron.* **16**, 274 (1986)].
- [14] R. S. Quimby and W. J. Miniscalco, *Appl. Opt.* **28**, 14 (1989).
- [15] M. A. Noginov, S. G. Semenov, V. A. Smirnov, and I. A. Shcherbakov, *Opt. Spektrosk.* **69**, 120 (1990) [*Opt. Spectrosc. (USSR)* **69**, 74 (1990)].
- [16] W. Lüthy and H. P. Weber, *Infrared Phys.* **32**, 283 (1991).
- [17] V. Lupei, S. Georgescu, and V. Florea, *IEEE J. Quantum Electron.* **29**, 426 (1993).
- [18] J. Rubin, A. Brenier, R. Moncorgé, and C. Pedrini, *J. Lumin.* **36**, 39 (1986).
- [19] C. Li, Y. Guyot, C. Linarès, R. Moncorgé, and M. F. Joubert, in *Advanced Solid-State Lasers and Compact Blue-Green Lasers Technical Digest, 1993* (Optical Society of America, Washington, DC, 1993), Vol. 2, pp. 423–425.
- [20] M. Pollnau, E. Heumann, and G. Huber, *Appl. Phys. A* **54**, 404 (1992).
- [21] W. Koechner, *Solid State Laser Engineering*, edited by A. L. Schawlow, K. Shimoda, A. E. Siegman, and T. Tamir, Springer Series in Optical Sciences Vol. 1 (Springer-Verlag, Berlin, 1988).
- [22] M. Pollnau, E. Heumann, and G. Huber, *J. Lumin.* **60+61**, 842 (1994).